ChemComm

Accepted Manuscript

This article can be cited before page numbers have been issued, to do this please use: Y. Luo, J. H. Tran, M. Wächtler, M. Schulz, K. Barthelmes, A. Winter, S. Rau, U. S. Schubert and B. Dietzek, *Chem. Commun.*, 2019, DOI: 10.1039/C8CC10075F.

View Article Online
DOI: 10.1039/C8CC10075F

Journal Name

COMMUNICATION

Remote control of electronic coupling – modification of excited-state electron-transfer rates in Ru(tpy)$_2$-based donor-acceptor systems by remote ligand design

Received 00th January 20xx,
Accepted 00th January 20xx

DOI: 10.1039/x0xx00000x

www.rsc.org/

Yusen Luo,[ab] Jens H. Tran,[a] Maria Wächtler,[ab] Kevin Barthelmes,[cd] Andreas Winter,[cd] Sven Rau,[e] Ulrich S. Schubert,[cd] and Benjamin Dietzek*[abd]

A comprehensive understanding of how the molecular structure influences the electronic coupling is crucial in optimizing (supra) molecular assemblies for photoinduced electron transfer. Here, we report that the electronic coupling underlying electron transfer from a phenothiazine donor to a photoexcited Ru(tpy)$_2$ acceptor is modulated by substitution of the second (remote) tpy-ligand.

Photoinduced electron transfer is a fundamental process in natural and artificial photosynthesis.[1-4] Compared to natural photosynthesis where electron transfer proceeds with unity quantum efficiencies and long-lived charge-separated states (CSS) are generated,[4] the artificial (supra)molecular assemblies need to be optimized to achieve efficient electron transfer and to produce long-lived CSS.[4-7] Optimization of such man-made systems requires an in depth understanding of the interplay between molecular structure and key parameters for electron transfer, *i.e.* electronic coupling (H_{DA}), reorganization energy (λ) and driving force ($-\Delta G°$) according to the semi-classical Marcus theory.[1,3-5] While the impact of molecular structure on λ and $-\Delta G°$ is quite well understood[4,5,8,9] and / or can be estimated quite well from *e.g.* electrochemical measurements (see ESI for a more detailed description), the factors governing H_{DA} are not fully comprehended yet: The nature of electron donor (D) and electron acceptor (A), the structure of molecular spacers (*e.g.* length[1,3,10,11] and substituents[12-17]) separating D and A as well as the molecular conformation[18-21] have significant effects on H_{DA}: H_{DA} generally decreases with increasing D–A distance.[1,3,10,11] Carbonera and coworkers pointed out that substitution of a molecular spacer in structurally related carotenoid–porphyrin–fullerene triads increased H_{DA} and, thus, significantly increased the charge recombination rate.[13] Albinsson and coworkers reported conformer-dependent electron-transfer rates in a (Zinc porphyrin)$_2$–fullerene dyad.[20] The significantly different electron-transfer rates for different molecular conformers were ascribed to the significantly different H_{DA} in the two conformers.[20] Despite these and other careful studies on the structural impact on the electron-transfer rates[1,3,4,10-18] it is difficult to isolate the impact of various structural factors on H_{DA} in photoactive transition metal complexes based D–A systems: Altering *e.g.* the chemical nature of D or A will impact not only electronic coupling but also the driving force for electron transfer.

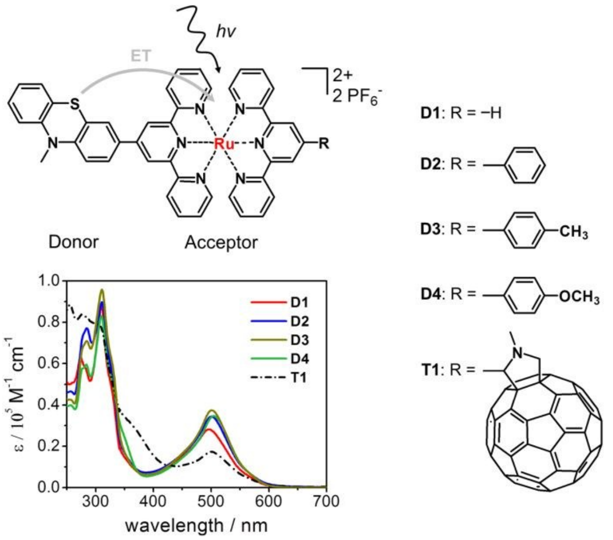

Fig 1. Molecular dyads **D1–D4** and triad **T1** studied in this work. Upon excitation of Ru^{II}(tpy)$_2$ center, electron transfer (ET) takes place from phenothiazine (PTZ) donor to photo-oxidized Ru(II) in the Ru(tpy)$_2$ center.[23,24] This process is of particular interest and we will focus on it in this work. For detailed decay processes after photoexcitation see Fig. S1. The UV-Vis absorption spectra shown here were recorded at room temperature in dichloromethane. For **D1** and **T1** the spectra were taken from ref 22.

---

[a] *Institute of Physical Chemistry and Abbe Center of Photonics, Friedrich Schiller University Jena, Helmholtzweg 4, 07743 Jena, Germany*
[b] *Department Functional Interfaces, Leibniz Institute of Photonic Technology (IPHT), Albert-Einstein-Straβe 9, 07745 Jena, Germany.*
E-mail: benjamin.dietzek@leibniz-ipht.de
[c] *Laboratory of Organic and Macromolecular Chemistry (IOMC), Friedrich Schiller University Jena, Humboldtstraβe 10, 07743 Jena, Germany*
[d] *Center for Energy and Environmental Chemistry Jena (CEEC Jena), Friedrich Schiller University Jena, Philosophenweg 7a, 07743 Jena, Germany*
[e] *Institute for Inorganic Chemistry I, Ulm University, Albert-Einstein-Allee 11, 89081 Ulm, Germany*

Electronic Supplementary Information (ESI) available: [details of any supplementary information available should be included here]. See DOI: 10.1039/x0xx00000x

View Article Online
DOI: 10.1039/C8CC10075F

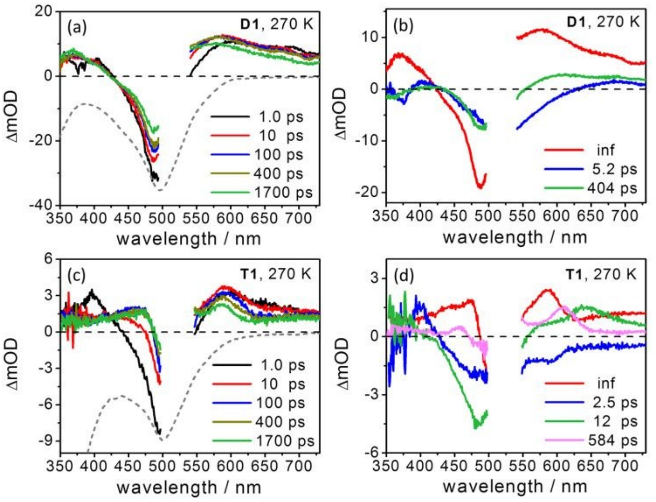

Fig 2. (a, c) fs TA spectra at selected delay times and (b, d) decay-associated spectra resulting from the global fit of fs TA data collected in a 1 cm cuvette in dichloromethane at 270 K for **D1** (a, b) and **T1** (c, d). The grey dashed line represents the shape of the corresponding inverted ground state absorption spectrum which is scaled to fit the respective figure.

In this contribution, we discuss how electronic coupling underlying the photoinduced electron transfer in a phenothiazine donor–Ru(tpy)$_2$ acceptor complex (*i.e.* **D1**, Fig. 1) can be modified without changing the D–A distance or the chemical nature of the linkage. Tuning H_{DA} is simply achieved by modifying the substituents at the 4'-position of the remote terpyridine ligand (*i.e.* –R, Fig. 1). This ligand does not link the photoactive Ru(II) core to the phenothiazine donor, and hence, it presents a convenient handle to tune the electronic coupling within the paradigm D–A dyad. We vary the substituent R from H atom to C_{60}, phenyl and more extended phenylmethyl, phenylmethoxy and show that H_{DA} values in the systems change significantly albeit similar driving forces, fixed chemical nature of D and identical D–A linkage and consequently fixed distance and mutual arrangement of D and A.

To quantify the H_{DA} values temperature-dependent electron-transfer rates were determined between 300 and 240 K by transient absorption spectroscopy (see Fig. S2–S11 for the full sets of data): The Ru(tpy)$_2$-core was excited at 520 nm, *i.e.* the red edge of the MLCT band. For each of the compounds, the TA spectra do not change significantly upon decreasing the temperatures. Hence, the previously developed model to account for the photoinduced processes in **D1** and **T1** at room temperature (Fig. S1)[23,24] is applied to analyze the temperature-dependent data. Fig. 2 exemplarily show the fs TA spectra of **D1** and **T1** at 270 K: At short delay times, the spectra are dominated by strong ground state bleach (GSB) at around 500 nm and two excited-state absorption (ESA) bands below 450 nm and above 550 nm. At long delay times, *e.g.* at 1700 ps for **D1**, the ESA band shifts from 600 to 580 nm meanwhile a new ESA band appears at 365 nm (Fig. 2a). Both features are indicative of the formation of one-electron oxidized phenothiazine ($PTZ^{\cdot+}$) according to spectroelectrochemistry revealing three distinct absorption bands at 365, 473 and 580 nm for $PTZ^{\cdot+}$.[23] The band at 473 nm is not prominent in **D1** (Fig. 2a) which is due to the spectral overlap with the residual GSB. These observations agree with our previous reports on **D1** at room temperature[23] and indicate an electron transfer from the PTZ donor to the excited acceptor Ru(tpy)$_2$*, *i.e.* the formation of $PTZ^{\cdot+}$–Ru(tpy)$_2^{\cdot-}$. For **T1** at 1700 ps, two distinct ESA bands are observed at 475, 585 and a rather broad feature at around 700 nm (Fig. 2c). The two bands are assigned to the absorption of $PTZ^{\cdot+}$ and the far-red feature is attributed to the absorption of the fullerene triplet state ($^3C_{60}$*). Different to **D1** (Fig. 2a), the absorption band of $PTZ^{\cdot+}$ at 365 nm is not pronounced in fs TA spectra of **T1** (Fig. 2c) due to the spectral overlap with the negative absorption of reduced fullerene ($C_{60}^{\cdot-}$) below 400 nm.[23] Hence, in **T1** the fully charge-separated state, $PTZ^{\cdot+}$–Ru(tpy)$_2$–$C_{60}^{\cdot-}$, is formed.

Temperature-dependent electron-transfer time constants were obtained by global fits of the fs TA data (see Fig. 2b, d, Fig. S3, S5, S7, S9 and S11). Previous experiments combining transient absorption and resonance Raman spectroscopy showed that the processes associated with τ_1 and τ_2 (Fig. 2b, d) occur from two distinct ^{3}MLCT states (Fig. S1).[23] The first kinetic component (τ_1) is characterized by an increased absorption at 365 nm and at 550 to 590 nm corresponding to the absorption of $PTZ^{\cdot+}$.[23] Thus, the respective kinetic component is attributed to the PTZ→Ru(tpy)$_2$* electron transfer. It should be noted that the characteristic time constant of the electron transfer is in the same range as previously described rotational motion around the terpyridine-phenyl (tpy-ph) bond (typically also observed on a some-ps timescale for Ru(tpy)$_2$-derived systems[25-27]). This indicates that the PTZ→Ru(tpy)$_2$* electron transfer is likely accompanied by planarization of the tpy-ph ligand in **D2**–**D4**. The second component (τ_2) represents the relaxation of ^{3}MLCT state localized on the terminal tpy ligand, *i.e.* a $^3MLCT_{tpy\text{-}R}$ state: For **D1**–**D4** it deactivates directly to ground state. For **T1** $^3MLCT_{tpy\text{-}R}$ undergoes an energy transfer yielding a $^3C_{60}$* state.[23] The third component in **T1** is attributed to the formation of $PTZ^{\cdot+}$–Ru(tpy)$_2$–$C_{60}^{\cdot-}$.[23,24] To investigate how intramolecular electronic coupling is influenced by substitution of the remote ligand, we focus on the PTZ→Ru(tpy)$_2$* electron transfer for which all compounds have the same D and D–A distance.

To obtain H_{DA} values for the photoinduced electron transfer PTZ→Ru(tpy)$_2$*, the Marcus equation was used:[28-32]

$$\ln\left(k_{ET}\cdot T^{\frac{1}{2}}\right)=\ln\left(\sqrt{\frac{\pi}{\hbar^2\cdot\lambda\cdot k_B}}\cdot {H_{DA}}^2\right)-\frac{(\lambda+\Delta G^\circ)^2}{4\cdot\lambda\cdot k_B\cdot T}\qquad(1)$$

Plotting $\ln(k_{ET}\cdot T^{1/2})$ *vs.* 1/T yields a straight line (see Fig. 3b) indicating that both λ and $(\lambda+\Delta G^\circ)^2/4\lambda$ are temperature-independent.[33,34] This is in line with the estimated λ (according to Marcus' dielectric continuum model) and $-\Delta G^\circ$ in the temperature region of 300 to 240 K that λ and the term $(\lambda+\Delta G^\circ)^2/4\lambda$ (*i.e.* the activation energy barrier $\Delta G^\ddagger$) are nearly temperature independent (see Table S3–4). Recently, Wenger showed experimentally that $-\Delta G^\circ$ is indeed temperature independent in a related donor-photosensitizer-acceptor system.[35] Under such conditions λ and H_{DA} can be extracted from the slope and the intercept of the linear regression, respectively.[28,29] Experimentally, τ_1 increases with decreasing temperature (Fig. 3a and Table S1) indicating reduced electron-transfer rates (k_{ET}) at lower temperatures. The full set of parameters describing electron transfer within Marcus' theory, *i.e.* λ, $-\Delta G^\circ$, H_{DA} and $\Delta G^\ddagger$ extracted from Fig. 3b, is summarized in Table 1.

Table 1. Summary of driving force ($-\Delta G^\circ$), reorganization energy (λ), electronic coupling (H_{DA}) and activation energy barrier ($\Delta G^\ddagger$) obtained from the experimental results shown in Fig. 3b for the PTZ→Ru(tpy)$_2$* electron transfer process in **D1**–**D4** and **T1**.

	D1	D2	D3	D4	T1
$-\Delta G^\circ$ / eV	0.29[a]	0.26[b]	0.25[b]	0.24[b]	0.23[a]
λ / eV	0.72	0.67	0.65	0.95	0.71
H_{DA} / cm^{-1}	94	90	74	371	157
$\Delta G^\ddagger$ / eV	0.064	0.063	0.062	0.13	0.072

[a] Values were taken from ref 24. [b] Values were obtained from the electrochemical data (Fig. S12) according to Rehm-Weller equation (eq S3-4).

$-\Delta G^\circ$ for PTZ→Ru(tpy)$_2$* electron transfer varies by only 20% within the investigated series from 0.29 (**D1**) to 0.23 eV (**T1**). Likewise, due to identical D, D–A distance and mutual D–A orientation the reorganization energy (λ) is rather similar for **D1**–**D3** and **T1** varying from 0.65 (**D3**) to 0.72 eV (**D1**). However, **D4** exhibits a roughly 40% higher λ which indicates that the inner-sphere reorganization energy λ_i must be significantly changed, as the outer-sphere reorganization energy λ_o is not supposed to vary a lot within the assumptions of the dielectric continuum model (eq S1–2). In contrast to λ and $-\Delta G^\circ$, H_{DA} values are quite different within the series of complexes investigated. They vary by more than 400% from **D3** to **D4** despite of minimal structural differences (see Table 1): **D4**, with the strongly electron-donating substituent $-OCH_3$, shows the strongest coupling (371 cm^{-1}); **T1** with the directly connected strongly electron withdrawing $-C_{60}$ reveals moderate coupling (157 cm^{-1}); For **D1**–**D3** the H_{DA} values are significantly lower (*i.e.* between 90 and 70 cm^{-1}). Thus, for example, replacing the –H atom at the 4'-position of the terminal tpy ligand in **D1** by $-C_{60}$ (*i.e.* **T1**) causes a roughly 70% increase of H_{DA} between PTZ and Ru(tpy)$_2$* despite the fact that **D1** and **T1** have the same D, D–A linkage and D–A distance. The electron rich $-OCH_3$ group in *para* position of the phenyl ring increases the coupling by a factor of 3 comparing **D2** and **D4**.

Similar effects have been reported for mixed-valance Ru^{II}/Ru^{III} complexes.[36,37] Here, the properties of intervalence charge-transfer (IVCT) transitions were altered by design of remote ligands: While this strategy ensured almost identical driving forces in a broad range of substitutions the electronic coupling underlying the IVCT could be altered by 20%. However, this work[36] does not consider photoinduced excited-state electron-transfer reactions in the mixed-valence systems.

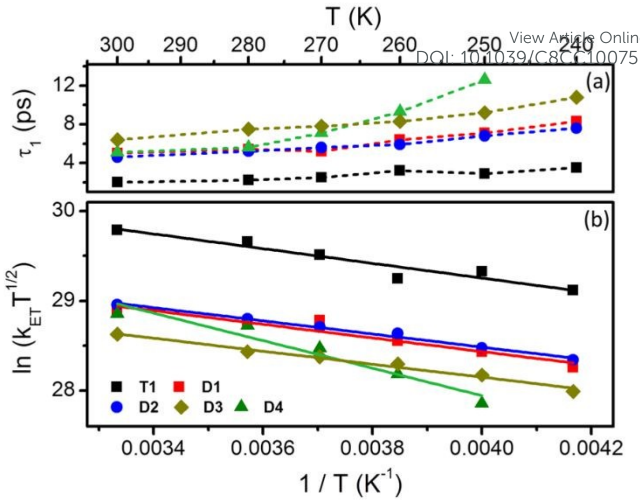

Fig 3. (a) Temperature dependence of the time constant associated with PTZ→Ru(tpy)$_2$* electron transfer. The dashed lines are only guides to the reader. (b) Plots of ln ($k_{ET}\cdot T^{1/2}$) *vs.* 1/T for **D1**–**D4** and **T1** with the corresponding linear fit. The adjusted R^2 value of the linear fit is 0.90 (**D1**), 0.99 (**D2**), 0.98 (**D3**), 0.92 (**D4**) and 0.90 (**T1**).

To rationalize the control of the donor-acceptor coupling by remote ligand design, we will consider the influence of the substituents –R on the charge densities. Such consideration is based on the fact that H_{DA} will be largely determined by the electronic structure of the molecular fragments involved.[38] Previously published calculations have studied the ground[39] and ^{1}MLCT excited-states[40] of two model Ru(tpy)$_2$ complexes with strongly electron donating ($-NH_2$) and electron withdrawing ($-NO_2$) groups attached to the 4'-position of the tpy ligand via a phenyl spacer (ph, see Fig. S13).[39,40] Calculations showed an increased π-character and a consequently shortened tpy-ph bond upon introducing the $-NH_2$ substituent. Furthermore, the electron donating group reduces the dihedral angle between ph and tpy in the ground state of the complex.[39] The $-NO_2$ facilitates long-range charge delocalization both in the ground- and excited-state albeit a larger tpy-ph dihedral angle in the ground state.[39,40] Similar effects on the electronic levels of a Ru(II) complex were calculated by Kupfer, who considered the effect of coligand exchange on the electronics of charge-accumulation within a photoactive Ru(II)-complex.[41]

The above discussed literature details the impact of substituents on the electronic situation in related Ru(II) complexes, leaving the question unanswered if such substitutions can be utilized to affect electronic coupling of the photoactive Ru(II) core with an electron donor linked via a second non-modified ligand. Comparing the PTZ-Ru(tpy)$_2$* electronic coupling within the series of complexes investigated here, will address this issue (to the best of our knowledge for the first time in a systematic experimental approach). Within the series of the dyads investigated the electron rich $-OCH_3$ substituent drastically increases the PTZ-Ru(tpy)$_2$* coupling as reflected in the H_{DA} value. This is accompanied by a significant increase of λ associated with the PTZ→Ru(tpy)$_2$* electron transfer. This increase in λ is likely associated with a decreased tpy-ph bond length and smaller tpy-ph dihedral angle in **D4** as λ_i can be related to the free energy change associated with bond length changes[42] which upon electron transfer would be different. Thus, the electron rich $-OCH_3$ substituent in **D4** leads to structural changes within the modified (remote) tpy ligand affecting λ but also to electronic changes altering the electronic coupling underlying PTZ-Ru(tpy)$_2$* electron transfer.

View Article Online
DOI: 10.1039/C8CC10075F

The slight (~18%) decrease in H_{DA} comparing **D3** to **D2** might stem from the weak electron-donating ability of the CH_3 group. This property causes the tpy-ph unit to be more planar than in **D2**.[39] Consequently, upon photoexcitation of the $Ru(tpy)_2$-photocenter in its MLCT transition, the access charge on the formally reduced ligand(s) becomes somewhat more delocalized, hence, reducing the coupling for the PTZ→ $Ru(tpy)_2$* electron transfer. Alterations of the remote ligand upon introduction of C_{60}, *i.e.* comparing **D1** and **T1**, increases H_{DA} by 70%. The effect of the C_{60}-containing tpy ligand also shifts the Ru^{III}/Ru^{II} oxidation anodically by 120 mV compared to **D1** (Table S2). The shifted HOMO apparently impacts the electronic levels on the PTZ-tpy ligand and thus increases the coupling underlying the PTZ→$Ru(tpy)_2$* electron transfer.

An experimental investigation on the electronic coupling underlying the photoinduced electron transfer in D–A dyads of the form PTZ–(tpy)Ru(tpy–R) is presented. The data reveal the possibility to modulate H_{DA} between the PTZ donor and the Ru(II) acceptor/photosensitizer by a factor of four by changing the remote substituent –R. Altering the electronics in the photo-excited $Ru(tpy)_2$*-photosensitizer, either by delocalization of the relaxed excited-state within the ligand sphere or by modifying the HOMO level of the Ru(II) ion, impacts the electronic coupling for photoinduced electron transfer in the dyad. Thus, the data point towards an additional design parameter for molecular systems, in which realizing efficient and specific electron transfer paths is key to improved function.

Acknowledgments

This research is supported by the China Scholarship Council.

Conflicts of interest

There are no conflicts to declare.

Notes and references

1 M. Natali, S. Campagna and F. Scandola, *Chem. Soc. Rev.*, 2014, **43**, 4005–4018.
2 M. D. Kärkäs, O. Verho, E. V. Johnston and B. Åkermark, *Chem. Rev.*, 2014, **114**, 11863–12001.
3 M. Gilbert and B. Albinsson, *Chem. Soc. Rev.*, 2015, **44**, 845–862.
4 M. Rudolf, S. V. Kirner and D. M. Guldi, *Chem. Soc. Rev.*, 2016, **45**, 612–630.
5 S. Fukuzumi, K. Ohkubo and T. Suenobu, *Acc. Chem. Res.*, 2014, **47**, 1455–1464.
6 K. A. Mazzio and C. K. Luscombe, *Chem. Soc. Rev.*, 2015, **44**, 78–90.
7 L. Hammarström, *Faraday Discuss.*, 2017, **198**, 549–560.
8 P. Vath and M. B. Zimmt, *J. Phys. Chem. A*, 2000, **104**, 2626–2633.
9 C. Schubert, J. T. Margraf, T. Clark and D. M. Guldi, *Chem. Soc. Rev.*, 2015, **44**, 988–998.
10 M. Kuss-Petermann and O. S. Wenger, *Angew. Chem. Int. Ed.*, 2016, **55**, 815–819.
11 T. Higashino, T. Yamada, M. Yamamoto, A. Furube, N. V. Tkachenko, T. Miura, Y. Kobori, R. Jono, K. Yamashita and H. Imahori, *Angew. Chem. Int. Ed.*, 2016, **55**, 629–633.
12 C. Lambert, G. Nöll and J. Schelter, *Nat. Mater.*, 2002, **1**, 69–73.
13 M. D. Valentin, A. Bisol, G. Agostini and D. Carbonera, *J. Chem. Inf. Model.*, 2005, **45**, 1580–1588.
14 M. P. Eng and B. Albinsson, *Chem. Phys.*, 2009, **357**, 132–139.
15 R. N. Sampaio, E. J. Piechota, L. Troian-Gautier, A. B. Maurer, K. Hu, P. A. Schauer, A. D. Blair, C. P. Berlinguette and G. J. Meyer, *Proc. Natl. Acad. Sci. U.S.A.*, 2018, **115**, 7248–7253.
16 S. E. Miller, A. S. Lukas, E. Marsh, P. Bushard and M. R. Wasielewski, *J. Am. Chem. Soc.*, 2000, **122**, 7802–7810.
17 M. E. Walther and O. S. Wenger, *ChemPhysChem*, 2009, **10**, 1203–1206.
18 Y. Zhao, X. Li, Z. Wang, W. Yang, K. Chen, J. Zhao and G. G. Gurzadyan, *J. Phys. Chem. C*, 2018, **122**, 3756–3772.
19 A. C. Benniston, A. Harriman, P. Li , P. V. Patel and C. A. Sams, *Phys. Chem. Chem. Phys.*, 2005, **7**, 3677–3679.
20 M. U. Winters, J. Kärnbratt, H. E. Blades, C. J. Wilson, M. J. Frampton, H. L. Anderson and B. Albinsson, *Chem. Eur. J.*, 2007, **13**, 7385–7394.
21 D. M. Guldi, A. Hirsch, M. Scheloske, E. Dietel, A. Troisi, F. Zerbetto and M. Prato, *Chem. Eur. J.*, 2003, **9**, 4968–4979.
22 K. Barthelmes, A. Winter and U. S. Schubert, *Eur. J. Inorg. Chem.*, 2016, **2016**, 5132–5142.
23 Y. Luo, K. Barthelmes, M. Wächtler, A. Winter, U. S. Schubert and B. Dietzek, *Chem. Eur. J.*, 2017, **23**, 4917–4922.
24 Y. Luo, K. Barthelmes, M. Wächtler, A. Winter, U. S. Schubert and B. Dietzek, *J. Phys. Chem. C*, 2017, **121**, 9220–9229.
25 P. P. Laine, F. Bedioui, F. Loiseau, C. Chiorboli and S. Campagna, *J. Am. Chem. Soc.*, 2006, **128**, 7510–7521.
26 K. Barthelmes, J. Kübel, A. Winter, M. Wächtler, C. Friebe, B. Dietzek and U. S. Schubert, *Inorg. Chem.*, 2015, **54**, 3159–3171.
27 R. Siebert, D. Akimov, M. Schmitt, A**.** Winter, U. S. Schubert, B. Dietzek and J. Popp, *ChemPhysChem*, 2009, **10**, 910–919.
28 M. G. Gatty, A. Kahnt, L. J. Esdaile, M. Hutin, H. L. Anderson and B. Albinsson, *J. Phys. Chem. B*, 2015, **119**, 7598–7611.
29 A. Kahnt, J. Kärnbratt, L. J. Esdaile, M. Hutin, K. Sawada, H. L. Anderson and B. Albinsson, *J. Am. Chem. Soc.*, 2011, **133**, 9863–9871.
30 F. Giacalone, J. L. Segura, N. Martín and D. M. Guldi, *J. Am. Chem. Soc.*, 2004, **126**, 5340–5341.
31 A. M. Scott and M. R. Wasielewski, *J. Am. Chem. Soc.*, 2011, **133**, 3005–3013.
32 M. Kuss-Petermann and O. S. Wenger, *J. Am. Chem. Soc.*, 2016, **138**, 1349–1358.
33 J. Kroon, H. Oevering, J. W. Verhoeven, J. M. Warman, A. M. Oliver and M. N. Paddon-Row, *J. Phys. Chem.*, 1993, **97**, 5065–5069.
34 R. H. Goldsmith, O. DeLeon, T. M. Wilson, D. Finkelstein-Shapiro, M. A. Ratner and M. R. Wasielewski, *J. Phys. Chem. A*, 2008, **112**, 4410–4414.
35 S. Neumann and O. S. Wenger, *Inorg. Chem.*, 2019, **58**, 855–860.
36 J.-Y. Shao and Y.-W. Zhong, *Chem. Eur. J.*, 2014, **20**, 8702–8713.
37 Y.-W. Zhong, Z.-L. Gong, J.-Y. Shao and J. Yao, *Coord. Chem. Rev.*, 2016, **312**, 22–40.
38 C.-P. Hsu, *Acc. Chem. Res.*, 2009, **42**, 509–518.
39 M. Presselt, B. Dietzek, M. Schmitt, S. Rau, A. Winter, M. Jäger, U. S. Schubert and J. Popp, *J. Phys. Chem. A*, 2010, **114**, 13163–13174.
40 J. Preiß, M. Jäger, S. Rau, B. Dietzek, J. Popp, T. Martínez and M. Presselt, *ChemPhysChem*, 2015, **16**, 1395–1404.
41 S. Kupfer, *Phys. Chem. Chem. Phys.*, 2016, **18**, 13357–13367.
42 G. J. Kavarnos and N. J. Turro, *Chem. Rev.*, 1986, **86**, 401–449.